JOURNAL OF VIROLOGY, Jan. 2002, p. 473–483 Vol. 76, No. 2
0022-538X/02/$04.00+0 DOI: 10.1128/JVI.76.2.473–483.2002


# The p23 Protein of *Citrus Tristeza Virus* Controls Asymmetrical RNA Accumulation†

Tatineni Satyanarayana, Siddarame Gowda, María A. Ayllón, María R. Albiach-Martí, Shailaja Rabindran, and William O. Dawson*

*Citrus Research and Education Center, University of Florida, Lake Alfred, Florida 33850*

Received 23 August 2001/Accepted 11 October 2001

***Citrus tristeza virus*** **(CTV), a member of the *Closteroviridae*, has a 19.3-kb positive-stranded RNA genome that is organized into 12 open reading frames (ORFs) with the 10 3′ genes expressed via a nested set of nine or ten 3′-coterminal subgenomic mRNAs (sgRNAs). Relatively large amounts of negative-stranded RNAs complementary to both genomic and sgRNAs accumulate in infected cells. As is characteristic of RNA viruses, wild-type CTV produced more positive than negative strands, with the plus-to-minus ratios of genomic and sgRNAs estimated at 10 to 20:1 and 40 to 50:1, respectively. However, a mutant with all of the 3′ genes deleted replicated efficiently, but produced plus to minus strands at a markedly decreased ratio of 1 to 2:1. Deletion analysis of 3′-end genes revealed that the p23 ORF was involved in asymmetric RNA accumulation. A mutation which caused a frameshift after the fifth codon resulted in nearly symmetrical RNA accumulation, suggesting that the p23 protein, not a *cis*-acting element within the p23 ORF, controls asymmetric accumulation of CTV RNAs. Further in-frame deletion mutations in the p23 ORF suggested that amino acid residues 46 to 180, which contained RNA-binding and zinc finger domains, were indispensable for asymmetrical RNA accumulation, while the N-terminal 5 to 45 and C-terminal 181 to 209 amino acid residues were not absolutely required. Mutation of conserved cysteine residues to alanines in the zinc finger domain resulted in loss of activity of the p23 protein, suggesting involvement of the zinc finger in asymmetric RNA accumulation. The absence of p23 gene function was manifested by substantial increases in accumulation of negative-stranded RNAs and only modest decreases in positive-stranded RNAs. Moreover, the substantial decrease in the accumulation of negative-stranded coat protein (CP) sgRNA in the presence of the functional p23 gene resulted in a 12- to 15-fold increase in the expression of the CP gene. Apparently the excess negative-stranded sgRNA reduces the availability of the corresponding positive-stranded sgRNA as a messenger. Thus, the p23 protein controls asymmetric accumulation of CTV RNAs by downregulating negative-stranded RNA accumulation and indirectly increases expression of 3′ genes.**

Most positive-stranded RNA viruses of eukaryotes have multicistronic RNA molecules that must function within cells that utilize monocistronic mRNAs. To overcome the limitations imposed by the gene expression rules of the host, these viruses have evolved different gene expression strategies, such as proteolytic processing of polyproteins into functional proteins, readthrough of stop codons, ribosomal frameshifting to express C-terminal domains fused to the higher-expressed protein, and internal ribosome entry sites and subgenomic mRNAs (sgRNAs) for expression of genes in the 3′ portion of the genome.

The use of sgRNAs for the expression of viral genes is a common strategy employed by a variety of evolutionarily dissimilar positive-stranded RNA viruses and allows independent regulation of timing and amounts of different viral proteins. sgRNAs can be produced by different mechanisms: by initiation at internal promoter sequences on the genomic negative-stranded RNA, a process that resembles the recognition of DNA promoters by DNA-dependent RNA polymerases (1, 17, 31), and by termination during negative-strand synthesis and transcription of mRNAs from the subgenomic template (25, 28, 29, 32).

*Citrus tristeza virus* (CTV), a member of the *Closterovirus* genus of the *Closteroviridae*, has a single-stranded, positive-sense RNA genome of 19.3 kb that is organized into 12 open reading frames (ORFs) (11, 20). The 5′-proximal ORFs 1a and 1b are translated from the genomic RNA. ORF 1a encodes a 349-kDa polyprotein containing two papain-like protease domains plus methyltransferase-like and helicase-like domains. ORF 1b encodes an RNA-dependent RNA polymerase-like domain that is thought to be translated by a +1 frameshift that continues translation, producing a ≈400-kDa polyprotein (11).

Ten 3′ ORFs are expressed through a series of 3′-coterminal sgRNAs (9) (Fig. 1A, CTV9). Temporal and quantitative regulation of transcription of CTV sgRNAs results in expression of some sgRNAs early and in large amounts (19). The 3′-most sgRNA, which encodes a 23-kDa RNA-binding protein (15), accumulates earliest (19). Higher levels of transcription tend to be associated with positions nearer the 3′ terminus, but the different levels of transcription of CTV sgRNAs are not strictly related to position in the genome. For example, the more abundantly transcribed sgRNAs result from positions 1 (p23), 2 (p20), and 5 (CP) from the 3′ terminus of the genome, while others are transcribed less abundantly (19, 22) (also see Fig. 1C, CTV9).

* Corresponding author. Mailing address: Citrus Research and Education Center, 700 Experiment Station Rd., Lake Alfred, FL 33850. Phone: (863) 956-1151. Fax: (863) 956-4631. E-mail: wodtmv@lal.ufl.edu.

† University of Florida Agricultural Experiment Station Journal Series R-08375.

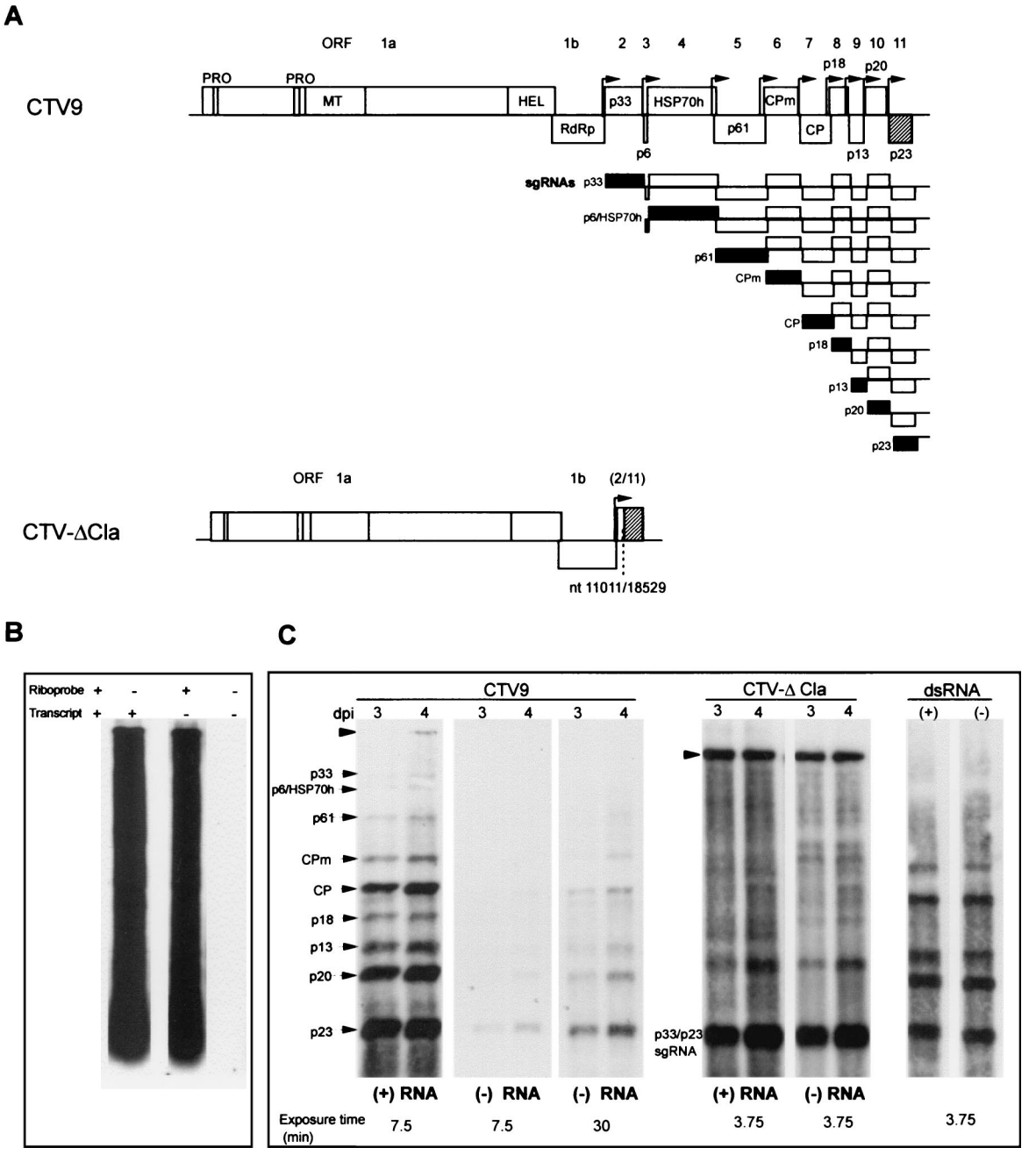


FIG. 1. Replication of wild-type CTV (CTV9) and deletion mutant CTV-ΔCla in *N. benthamiana* mesophyll protoplasts, showing accumulation of positive- and negative-stranded genomic and sgRNAs. (A) Schematic diagram of the genome organization and expression of 3′-terminal ORFs of CTV (CTV9) and CTV replicon CTV-ΔCla, showing the putative domains of papain-like proteases (PRO), methyltransferase (MT), helicase (HEL), and RNA-dependent RNA polymerase (RdRp) and ORFs (open boxes) with numbers and translation products. HSP70 h, HSP70 homolog; CPm, minor coat protein; CP, major coat protein; (2/11), represents fusion of ORFs 2 and 11. The nested set of sgRNAs are shown below the CTV genome organization, with the ORF presumably expressed from each sgRNA represented as a black box. The approximate positions of the 5′ termini of sgRNAs driven by controller elements for the respective ORFs are indicated by bent arrows at the 5′ end of each ORF. (B) Demonstration of the specificity of strand-specific riboprobes. Northern blot hybridizations of full-length plus-sense and nearly full-length (nt 3691 to 19296) minus-sense in vitro-produced RNA transcripts were hybridized with 3′ 900-nt positive- or negative-stranded digoxigenin-labeled RNA probes. Exposure times are identical. Reactive probes were greatly overexposed to show the degree of selectivity. Note that each probe hybridized to only the opposite-polarity RNA strands. (C) Northern blot hybridization of RNAs from protoplasts transfected with CTV9 and CTV-ΔCla at 3 and 4 dpi. Double-stranded RNA (dsRNA) from CTV-infected bark tissue was included in Northern blot hybridizations as a standard to equalize the strand-specific riboprobes. The positions of genomic and sgRNAs corresponding to ORFs 2 through 11 are indicated by arrowheads and arrows, respectively. The exposure time of blots is indicated at the bottom of the figure. Positive- and negative-stranded RNAs are indicated by (+) RNA and (−) RNA, respectively.

CTV sgRNAs appear to have properties intermediate between those of the "alphavirus-like supergroup" and the coronaviruses and arteriviruses of the *Nidovirales*. CTV has a large number (9 or 10) of 3′-coterminal sgRNAs, similar to coronaviruses (14, 30). However, CTV sgRNAs are contiguous with the genomic RNA (8, 12) similar to those of members of the alpha-like viruses (3, 17, 32), thus lacking the common 5′ leader of coronaviruses and arteriviruses.

In the alpha-like viruses, sgRNAs are generally thought to be produced by internal initiation of transcription on the full-length negative strand (17). Although small amounts of corresponding negative- or double-stranded sgRNAs can be found among these viruses, we have shown that the labeling kinetics were not consistent with the idea that negative-stranded sgRNAs are templates for sgRNA synthesis (6). In contrast, the *Closteroviridae,* like the *Coronaviridae,* produce much larger amounts of negative-stranded sgRNAs. The labeling kinetics of coronavirus sgRNAs suggest that the negative strands are replicative templates for independent transcription of sgRNAs (2, 25), but the function of the CTV negative-stranded sgRNAs remains unknown (8).

There is little information concerning the regulation of positive versus negative strands of sgRNAs, although there is information related to the ratios of these genomic RNAs. The genomic RNAs of positive-stranded RNA viruses generally are produced with a large excess of positive to negative strands. For example, the ratio is 10:1 for flaviviruses (4), 50 to 100:1 for coronaviruses (13), 100:1 for *Brome mosaic virus* (BMV) (7, 16), and 1,000:1 for *Alfalfa mosaic virus* (AMV) (18). Although we did not quantify the ratios previously, reexamination of the Northern hybridization blots (22) suggests plus-to-minus strand ratios in the range of 50:1 for wild-type CTV RNAs. Thus, CTV genomic RNA and its sgRNAs appear to fall within the range of the genomic RNAs of the above viruses in plus-to-minus strand ratios. In contrast, we noticed that mutants with all of the 3′ genes deleted replicated well but produced plus-to-minus strand ratios of nearly 1:1 (22).

Mechanisms that control the ratio of positive to negative strands of the genomic RNA of members of the alphavirus supergroup have been examined. In BMV, replication of RNAs 1 and 2 in the absence of RNA 3 results in a nearly 1:1 ratio of plus to minus strands (16). The addition of RNA3 enhanced the production of positive-stranded genomic RNAs 1 and 2 by 29-fold, whereas the negative-stranded RNAs decreased by only 4-fold. The central region of RNA 3 containing the sgRNA promoter was found to be the determinant for the enhanced plus-strand RNA accumulation. In AMV, a frameshift in the CP gene resulted in a 100-fold reduction in plus-strand RNA accumulation and a 3- to 10-fold increase in minus strand accumulation (34). *Sindbis virus* (SIN) replication consists of two phases, an initial exponential phase associated with a short-lived replication complex produces positive and negative strands of the genomic RNA in an approximately 1:1 ratio, and a linear phase that amplifies the positive-stranded genomic RNAs is associated with a stable replication complex (27). The N-domain of nonstructural protein (nsp) 2 of SIN plays an essential role in "conversion" from synthesis of templates to synthesis of progeny RNAs (26).

Here, we report the examination of factors affecting the accumulation of positive- and negative-stranded RNAs of CTV. Deletion mutagenesis revealed that the p23 gene was responsible for asymmetric accumulation of positive- and negative-stranded sgRNAs. Additionally, mutations in the p23 ORF suggested that the p23 protein regulated the accumulation of sgRNAs. The major effect of the p23 gene product appeared to be the downregulation of negative-stranded sgRNA accumulation with only a modest increase in positive-stranded sgRNA accumulation. Thus, alterations that caused CTV to produce plus-to-minus ratios of RNAs near unity resulted primarily from increased negative-stranded RNA accumulation rather than decreased positive-stranded RNA synthesis like the alpha-like viruses described above.

## MATERIALS AND METHODS

**Generation of CTV mutants.** The full-length cDNA clone pCTV9 and self-replicating deletion mutants pCTV-ΔCla and pCTV-ΔCla333 were described previously (Fig. 1) (8, 22). The nucleotide (nt) numbering and sequences of the primers used in this study are according to Karasev et al. (11), GenBank accession number NC001661. The deletion mutants CTV-Δp33-CPm, CTV-Δp33-p18, and CTV-Δp6-p20 were generated by digesting pCTV9 with *Pst*I (nt 11624) and *Sna*BI (nt 15790), *Pst*I (nt 11624 and 17208) or *Pme*I (nt 11872) and *Msc*I (nt 17946) restriction endonuclease enzymes, respectively, followed by religation (see Fig. 2A). When deletions were introduced by restriction enzyme digestion that created noncompatible ends, the single-stranded ends were blunt-ended with T4 DNA polymerase (New England Biolabs, Beverly, Mass.) prior to ligation.

CTV-p23, CTV-p20-p23, CTV-p13-p23, CTV-p18-p23, CTV-CP-p23, and CTV-CPm-p23 were generated by PCR-amplifying DNA fragments and ligating into CTV-ΔCla333 between the *Stu*I and *Not*I restriction endonuclease sites (see Fig. 3A). CTV-CPm-p20, CTV-CPm-p13, CTV-CPm-p18, and CTV-CPm-CP were obtained by ligating PCR-amplified DNA fragments between the *Xho*I and *Stu*I restriction endonuclease sites into CTV-ΔCla333 (see Fig. 4A). Deletions, frameshifts, and amino acid substitutions in the p23 ORF were introduced by PCR using mutagenic oligonucleotides, followed by overlap extension PCR (10) of the region between nt 18174 and 19296, comprising p23 sgRNA controller element sequences plus the p23 ORF. The PCR products were ligated into CTV-ΔCla333 between the *Xho*I and *Not*I restriction endonuclease sites. The region between nt 15898 and 16845, comprising the coat protein (CP) sgRNA controller element sequences plus the CP ORF, was ligated into CTV-ΔCla333 and CTV-p23 between the *Xho*I and *Stu*I and the *Xho*I and *Pst*I restriction sites to obtain CTV-CP and CTV-CP/p23, respectively. Deletions, frameshifts, and amino acid codon changes were confirmed by nucleotide sequencing.

**Protoplast transfection and Northern blot analysis of viral RNAs.** The procedures for the isolation of mesophyll protoplasts from *Nicotiana benthamiana* and polyethylene glycol-mediated transfections were carried out as described previously (22, 23). SP6 RNA polymerase-derived transcripts from CTV cDNAs were generated in vitro from *Not*I-linearized plasmids as described by Satyanarayana et al. (22). Protoplasts were harvested at 3 and 4 days postinoculation (dpi). The isolation of total nucleic acids from the pelleted protoplasts was carried out as described by Satyanarayana et al. (22). The 3′-terminal 900 nt of CTV-T36 in pGEM-7Zf (Promega) were used to make positive- and negative-stranded RNA-specific riboprobes with digoxigenin-labeled UTP using either SP6 or T7 RNA polymerase.

The accumulation of plus- and minus-stranded RNAs from $\approx 3 \times 10^4$ protoplasts transfected with CTV mutants was analyzed by Northern blot hybridizations using 3′-strand-specific riboprobes. Double-stranded RNA (≈100 ng) that consists of equal amounts of plus- and minus-strand RNAs from CTV-T36-infected bark tissue was included in Northern blot hybridizations to equalize the strand-specific riboprobes. The relative amounts of positive- and negative-stranded RNAs accumulated from CTV mutants were quantified at 4 dpi using different exposures of Northern blots by scanning and densitometry with the OS-SCAN program (Oberlin Scientific, Oberlin, Ohio). Results presented represent at least three to five independent protoplast transfections using two to three independent clones of each mutant.

**Immunoblot analysis.** Total protein from the phenolic phase of CTV-ΔCla-, CTV-CP-, and CTV-CP/p23-transfected protoplasts at 4 dpi was acetone precipitated. The immunoblot analysis of CTV CP was conducted using the ECL Western blotting system (Amersham Pharmacia Biotech, Piscataway, N.J.) and anti-CTV CP serum at a 1:5,000 dilution. Secondary goat anti-rabbit immuno-

globulin (Ig)-horseradish peroxidase-conjugated antibodies were used at a 1:2,000 dilution.

## RESULTS

**Production of CTV RNAs.** Accumulation of positive- and negative-stranded CTV genomic and sgRNAs was examined by comparing the wild-type virus to a series of deletion mutants derived from pCTV9 (22). *N. benthamiana* mesophyll protoplasts were inoculated with in vitro-produced RNA transcripts, followed by Northern blot hybridizations of progeny RNAs using 3′ positive- and negative-stranded RNA-specific riboprobes. The specificity of the riboprobes was demonstrated by hybridizing them to 0.5 μg of full-length or nearly full-length in vitro transcripts of each polarity of the viral RNA. Each probe hybridized to only the cRNA under the stringency conditions used for analysis of CTV RNAs from transfected protoplasts (Fig. 1B).

Wild-type CTV produced positive- and negative-sense genomic and nine distinguishable sgRNAs whose bands were visible in Northern blot hybridizations after long exposures (data not shown). However, the bands corresponding to the longer negative-stranded RNAs were not visible from exposures that clearly defined the smaller sgRNAs (Fig. 1C, CTV9). The ratios of positive- to negative-stranded RNAs were estimated for the genomic and the abundantly produced sgRNAs (CP, p20, and p23) at 4 dpi from Northern blot hybridization films of different exposures using double-stranded RNA preparations (Fig. 1C) as standards to equalize the strand-specific riboprobes. Genomic RNA appeared to accumulate at ratios of approximately 10 to 20:1 of plus to minus strands, whereas CP, p20, and p23 sgRNAs accumulated at a ratio of ≈40 to 50:1 positive to negative strands (Fig. 1C, CTV9).

However, while the smaller sgRNAs transferred from gels to membranes reliably, we were less confident of quantification of the genomic RNAs due to the difficulty of transferring ≈15- to 20-kb RNAs. Thus, we did not attempt to quantify the genomic RNA ratios in subsequent experiments, but general comparisons can be made by observing the Northern hybridization blots throughout the subsequent figures.

Previously we reported that the CTV replicon, CTV-ΔCla, in which all 3′ genes (p33-p23) are deleted, was capable of replication in protoplasts (Fig. 1) (22). CTV-ΔCla replicated efficiently, accumulating two RNA molecules detected by 3′ probes corresponding to the genomic RNA (≈11.8 kb) and a chimeric p33/p23 sgRNA (≈0.87 kb) (Fig. 1C, CTV-ΔCla). In several different experiments, the sgRNA of CTV-ΔCla accumulated at ratios between ≈1.5:1 and ≈2.5:1 of positive- to negative-stranded RNAs. The accumulation of positive strands of the chimeric sgRNA produced by CTV-ΔCla was similar to those of the most highly abundant sgRNAs of the wild-type virus (Fig. 1C), but the amount of corresponding negative strands of the sgRNA was considerably higher (≈70- to 80-fold). The near symmetry in the accumulation of positive- and negative-stranded sgRNAs of CTV-ΔCla appeared to result primarily from increased accumulation of the negative-stranded sgRNA (Fig. 1C, CTV-ΔCla).

**Mapping the region responsible for increased accumulation of negative-stranded sgRNAs.** Deletion of all of the 3′ genes of CTV, resulting in CTV-ΔCla, caused a large increase in the accumulation of negative-stranded RNAs to approximately the same level as that of the positive strands (Fig. 1A and 1C, CTV-ΔCla). We attempted to identify a smaller subset of sequences that, when deleted, caused the increased accumulation of negative-stranded sgRNAs (Fig. 2A). The progeny RNAs produced in protoplasts infected with mutants with a series of smaller deletions in the CTV genome were analyzed by Northern blot hybridizations using strand-specific riboprobes to detect the accumulation of positive- and negative-stranded sgRNAs.

Mutants CTV-Δp33-CPm, CTV-Δp33-p18, and CTV-Δp6-p20 replicated efficiently and accumulated positive- and negative-stranded sgRNAs in approximately similar amounts to that of the wild-type virus (Fig. 2B, a to c). We chose to quantify at 4 dpi the plus-to-minus strand ratios only for the p23 sgRNA from these deletion mutants because p23 is the only common ORF present in all the mutants. The plus-to-minus strand ratios of p23 sgRNA from CTV-Δp33-CPm, CTV-Δp33-p18, and CTV-Δp6-p20 were estimated to be 42:1, 35:1, and 37:1, respectively. Deletion mutant CTV-Δp33-p23 (CTV-ΔCla), in which the deletion extended into the p23 gene, replicated efficiently but produced plus- and minus-stranded sgRNAs at a ratio of 1.5:1 (Fig. 2B, d). A substantial increase in the accumulation of negative-stranded sgRNA was observed in CTV-Δp33-p23 (CTV-ΔCla) with no significant decrease in the accumulation of positive-stranded sgRNA compared to that of wild-type CTV and the other deletion mutants (Fig. 2B). These results suggested that the sequences in the 3′ region of the genome near the p23 ORF were probably responsible for the increased accumulation of negative-stranded sgRNAs.

**Examination of the role of 3′ genes in the accumulation of sgRNAs.** To determine whether sequences or ORFs more 5′ of the p23 gene affected sgRNA accumulation, we examined the effect of 3′ genes on the accumulation of minus-sense sgRNAs by inserting genes additively into a minimal derivative of CTV, CTV-ΔCla333. A segment of approximately 150 to 220 nt upstream of each ORF was included in each case with the expectation that these sequences would provide a controller element for synthesis of the sgRNA. The CTV replicon CTV-ΔCla333 replicates efficiently in protoplasts without producing any sgRNA (8).

CTV-p23 contained p23 ORF and 219 nt upstream of the p23 gene to provide the sgRNA controller element (Fig. 3A, a). In vitro-produced RNA transcripts of CTV-p23 were used to inoculate *N. benthamiana* protoplasts, resulting in accumulation of both plus- and minus-sense genomic and sgRNAs (Fig. 3B, a). The p23 sgRNA accumulated at a ratio of ≈30:1 positive- to negative-stranded sgRNA, which was only slightly less than that of the wild-type virus and much greater than that of CTV-ΔCla. The sgRNAs produced by CTV-p20-p23 and CTV-p13-p23, with one or two additional genes, consisted of relatively large amounts of positive strands and less negative strands (Fig. 3B, b and c). The positive-to-negative strand ratios of the p23 sgRNA of both mutants were estimated to be 34:1.

Mutants CTV-p18-p23, CTV-CP-p23, and CTV-CPm-p23 allowed examination of the effect of multiple genes on the accumulation of positive- and negative-stranded sgRNAs (Fig. 3A, d to f). These mutants replicated efficiently and produced genomic and sgRNAs of positive and negative polarity (Fig.

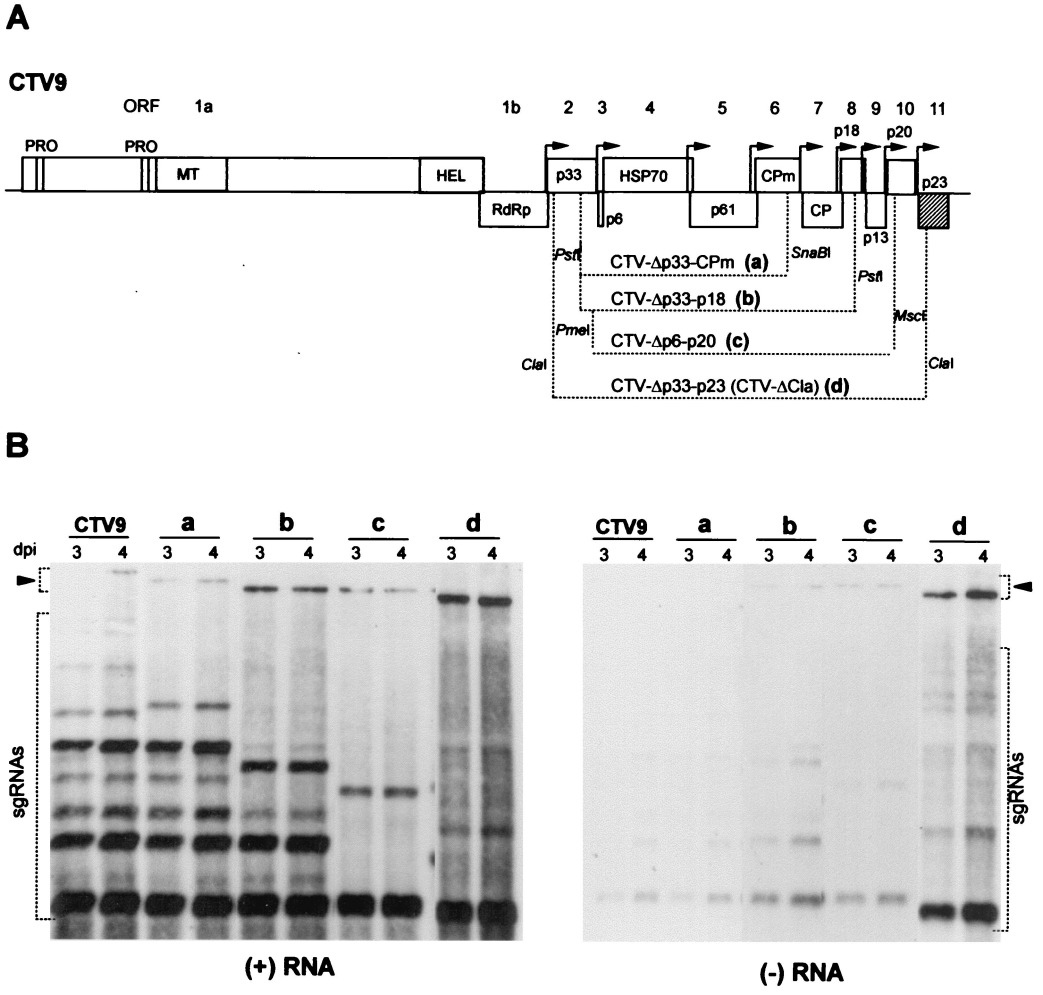


FIG. 2. Deletion mutations in 3′ ORFs of CTV to map the region involved in asymmetric accumulation of RNAs. (A) Schematic representation of the genome organization of wild-type CTV (CTV9) showing the deletion mutants CTV-Δp33-CPm (a), CTV-Δp33-p18 (b), CTV-Δp6-p20 (c), and CTV-Δp33-p23 (CTV-ΔCla) (d). The mutants were generated by deleting the sequences between the dotted lines using the indicated restriction enzymes. Bent arrows represent the approximate start position of sgRNAs. (B) Northern blot analysis of total RNAs from *N. benthamiana* protoplasts transfected with deletion mutants (a to d) at 3 and 4 dpi, showing the accumulation of positive- and negative-stranded genomic (arrowheads) and corresponding 3′-terminal sgRNAs using strand-specific riboprobes as described for Fig. 1.

3B, d to f), with positive-to-negative-strand ratios of the p23 sgRNA of ≈38 to 42:1, similar to that of wild-type CTV. Thus, the asymmetric accumulation of sgRNAs appeared to map to the p23 gene.

To examine whether other sgRNAs responded similarly to the presence or absence of the p23 region, we created a series of mutants with the 3′-most genes progressively deleted. We observed previously that smaller CTV RNAs more efficiently infect *N. benthamiana* protoplasts than do larger CTV RNAs (24). CTV-CPm-p23 (Fig. 3A, f) was used to generate mutants with progressive deletion of ORFs because it produced a plus-to-minus strand ratio of sgRNAs similar to that of the wild-type virus and its smaller size made it easier to manipulate and infect protoplasts than the full-genome RNA.

CTV-CPm-p20 contained the CPm, CP, p18, p13, and p20 genes and only the 3′ portion of the p23 ORF (the same portion contained in CTV-ΔCla, which does not produce p23 sgRNA because of loss of the p23 sgRNA controller element) (Fig. 4B, b). Analysis of positive- and negative-stranded sgRNAs accumulated from CTV-CPm-p20-transfected protoplasts revealed a reduction in asymmetric production of the sgRNAs due to a 12- to 15-fold increase in the accumulation of negative-stranded sgRNAs compared to CTV-CPm-p23. The p20 sgRNA ratio of positive to negative strands of CTV-CPm-p20 was 6:1 (Fig. 4B, compare a and b). CTV-CPm-p13, CTV-CPm-p18, and CTV-CPm-CP (Fig. 4A, c to e) replicated efficiently, with ratios of positive to negative strands of the sgRNAs closest to the 3′ end in all three constructs determined to be approximately 3 to 5:1.

The low plus-to-minus sense RNA ratio from the constructs without the p23 ORF was largely due to increased accumulation of negative-stranded sgRNAs, while the deletion of p23 and other 3′ genes had little effect on the accumulation of positive-stranded genomic or sgRNAs (Fig. 4B). Again, the major factor affecting sgRNA asymmetry was mapped to the p23 gene. (The increased signal of the genomic RNA of

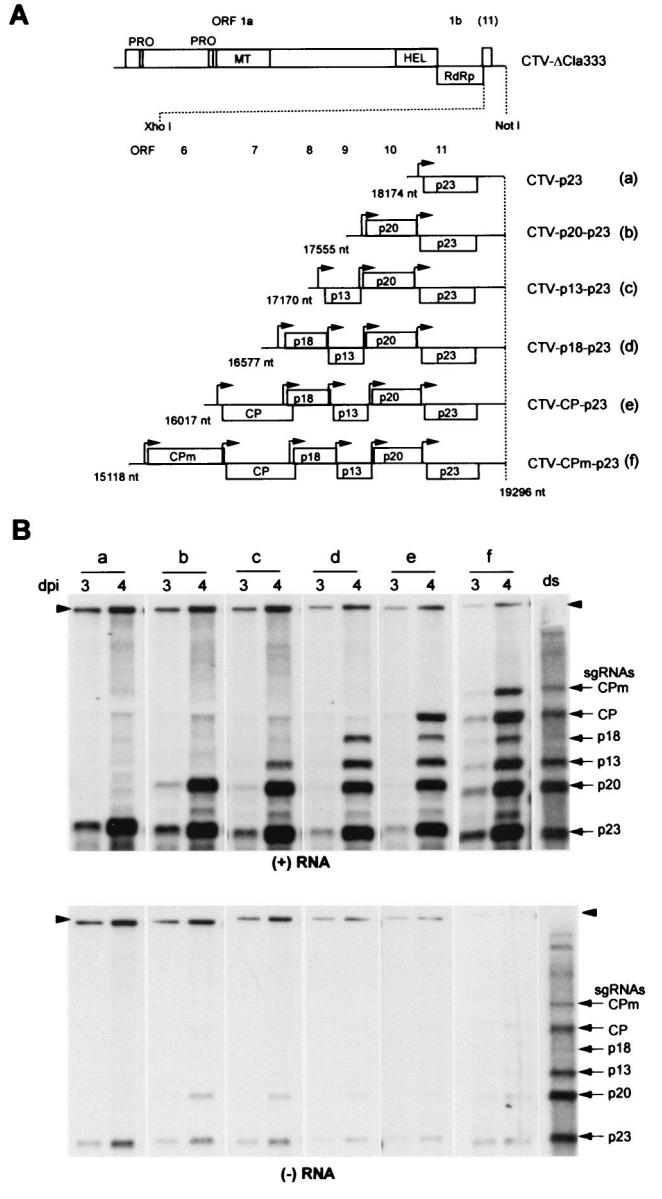


FIG. 3. Effect of 3′-most ORFs on the accumulation of positive- and negative-stranded RNAs by sequential addition of genes. (A) Schematic diagram of CTV-ΔCla333 and 3′ ORF(s) inserted additively from p23 to CPm into CTV-ΔCla333 between the *Xho*I and *Not*I restriction endonuclease sites (a to f). Nucleotide numbers represent the sequences present in CTV-ΔCla333. All insertions contained a constant 3′ end (nt 19296) and variable 5′ ends as indicated. Approximate positions of the 5′ termini of the sgRNAs are indicated with bent arrows. (B) Northern blot analysis of accumulation of positive- and negative-stranded RNAs from *N. benthamiana* protoplasts transfected with CTV mutants (a to f) at 3 and 4 dpi. The blots were hybridized with 3′ positive- and negative-stranded RNA-specific riboprobes along with double-stranded RNAs (ds) from CTV-infected plants as a standard to equalize strand-specific riboprobes. The positions of the genomic and corresponding sgRNAs of 3′-end genes are represented by arrowheads and arrows, respectively.

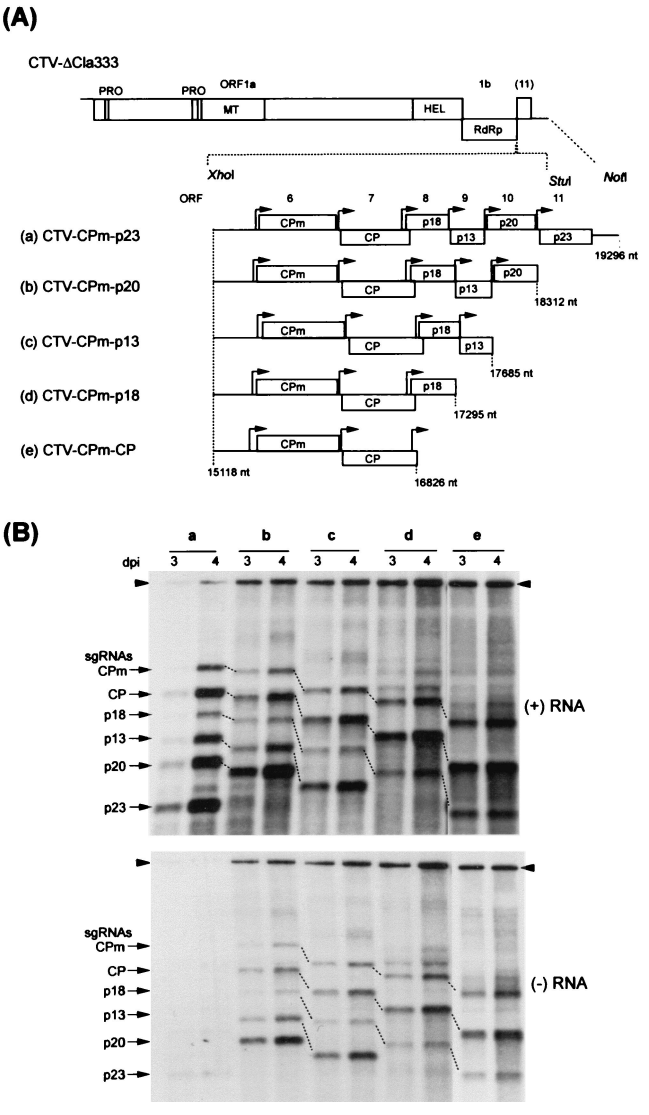


FIG. 4. Effect of presence or absence of p23 gene and sequential deletion of 3′-end genes on the accumulation of positive- and negative-stranded RNAs. (A) Schematic representation of mutants with sequential deletion of genes in CTV-CPm-p23 (a to e). The deletions were made by keeping a constant 5′ end (nt 15118) and variable 3′ ends as indicated. (B) Accumulation of positive- and negative-stranded RNAs from protoplasts transfected with mutants a to e at 3 and 4 dpi. Northern blots were hybridized with the 3′ positive- and negative-stranded RNA-specific riboprobes as described for Fig. 3. Genomic RNA and corresponding sgRNAs of 3′-end genes are represented by arrowheads and arrows, respectively. Dotted lines between lanes in Northern blots represent the corresponding sgRNA as shown to the left side of the blot.

smaller constructs in Fig. 4 was the result of the more efficient transfection of protoplasts by smaller CTV RNAs, as reported [24].)

To determine whether the effect of the p23 gene was uniform on all of the sgRNAs, we next examined full-length or nearly full-length CTV with and without the p23 gene. The mutant CTV9-Δp23 contained an in-frame deletion of 84 amino acid codons between nt 18532 and 18783 in the p23 gene with predicted translation of amino acids 1 to 46 and 131 to 209 of p23 (Fig. 5A). CTV9-Δp23 replicated and accumulated positive-stranded genomic and sgRNAs similar to CTV-Δp33 and wild-type CTV (23), but CTV9-Δp23 had a ≈10- to 15-fold

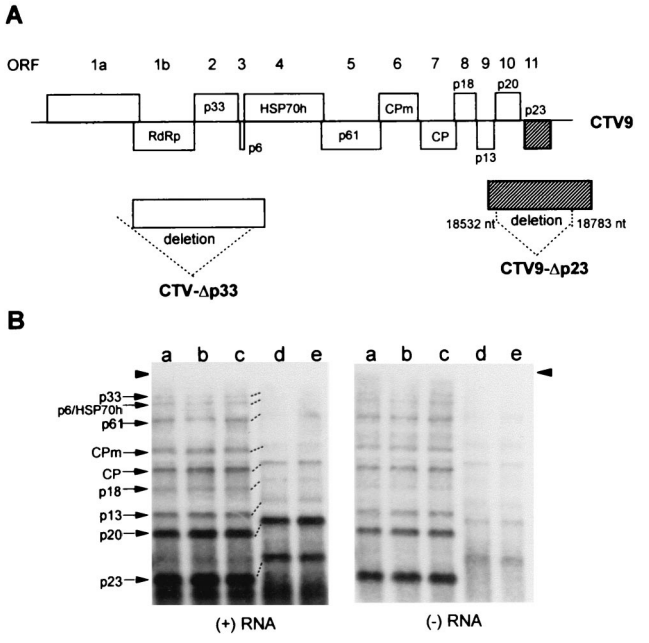


FIG. 5. Effect of p23 deletion in wild-type CTV (CTV9) on the accumulation of positive- and negative-stranded RNAs. (A) Genomic map of wild-type CTV9 (top part) and expanded view of p33 and p23 ORFs showing deletions made to obtain CTV-Δp33 (23) and CTV9-Δp23. (B) Northern blot analysis of accumulation of positive- and negative-stranded RNAs from CTV9-Δp23 (a to c, three independent clones), CTV-Δp33 (d), and wild-type CTV9 (e) at 4 dpi. Blots were hybridized with 3′ positive- and negative-stranded RNA-specific riboprobes. Genomic RNA and corresponding sgRNAs of 3′-end genes are indicated by arrowheads and arrows, respectively. sgRNAs from CTV9-Δp23 (a to c) migrated slightly faster than those from CTV-Δp33 (d) or wild-type CTV9 (e) due to a deletion in the p23 gene.

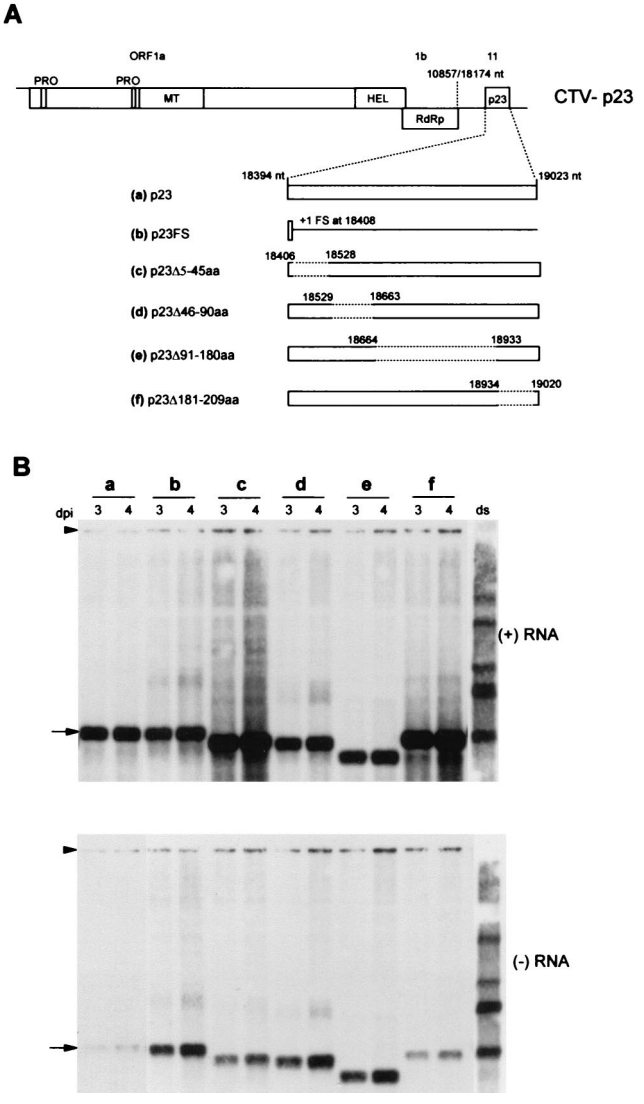


FIG. 6. Analysis of p23 gene function in asymmetric accumulation of sgRNAs. (A) Schematic diagram of CTV-p23 with a +1 frameshift (p23FS) at nt 18408, mutants with deletion of amino acids 5 to 45 (p23Δ5–45aa), 46 to 90 (p23Δ46–90aa), 91 to 180 (p23Δ91–180aa), and 181 to 209 (p23Δ181–209aa). Positions of deletions are indicated by dotted lines and corresponding nucleotide numbers. Boxes and solid lines represent translatable and nontranslatable sequences, respectively. (B) Northern blot analysis of accumulation of positive- and negative-stranded p23 sgRNAs from *N. benthamiana* protoplasts transfected with wild-type CTV-p23 (a), the frameshift mutant (b), and deletion mutants (c to f) at 3 and 4 dpi using 3′ positive- and negative-stranded RNA-specific riboprobes. Double-stranded RNA (ds) from CTV-infected plants was included in Northern blots as a standard to equalize strand-specific riboprobes. Positions of genomic RNA and p23 sgRNA are indicated by arrowheads and arrows, respectively.

increase in accumulation of negative-stranded sgRNAs (Fig. 5B).

**Putative role of p23 protein in sgRNA asymmetry.** To examine whether the p23 region functioned to downregulate negative-stranded sgRNA accumulation via a *cis*-acting RNA sequence or whether the p23 protein was needed, we made mutations in the p23 ORF to disrupt protein production or function with minimal disruption of a potential *cis*-acting RNA element. We generated mutant p23FS, which contained a +1 frameshift at nt 18408 with the addition of nucleotide U, which was predicted to result in the translation of only the first five native p23 codons followed by 10 nonviral codons. This mutant replicated efficiently and accumulated both positive- and negative-stranded sgRNAs (Fig. 6B, b). The frameshift in p23 resulted in a 23- to 30-fold increase in the accumulation of negative-stranded sgRNA over that of CTV-p23, whereas the accumulation of positive-stranded sgRNA was decreased by only ≈1- to 2-fold (Fig. 6B, b; Table 1). These results suggested that the p23 protein was responsible for the downregulation of the accumulation of minus-stranded sgRNAs.

To further examine the putative function of the p23 protein, a series of in-frame deletion mutants were examined. Two of the deletions were designed to remove the RNA binding domain which contained a predicted zinc finger domain (15). Mutant p23Δ5–45aa contained a deletion of amino acid codons 5 to 45 between nt 18406 and 18528. Mutant p23Δ46–90aa had a deletion of amino acid codons 46 to 90 between nt 18529 and 18663, and mutant p23Δ91–180aa contained a deletion between nt 18664 and 18933, encoding amino acids 91 to 180. The region between nt 18934 and 19020, encoding amino acids 181 to 209, was deleted to obtain p23Δ181–209aa (Fig. 6A). All these mutants replicated efficiently and produced genomic and sgRNAs of positive and negative polarity (Fig. 6B).

TABLE 1. Effect of frameshift and deletion mutations in p23 ORF on the accumulation of positive- and negative-stranded p23 sgRNAs from CTV-p23

| Construct | Plus-to-minus strand sgRNA ratio | | | Accumulation of sgRNA over wild-type level (fold change) | | | | | |
|---|---|---|---|---|---|---|---|---|---|
| | | | | Plus-strand sgRNA | | | Minus-strand sgRNA | | |
| | Expt 1 | Expt 2 | Expt 3 | Expt 1 | Expt 2 | Expt 3 | Expt 1 | Expt 2 | Expt 3 |
| CTV-p23 | 49:1 | 30:1 | 46:1 | | | | | | |
| p23FS | 1.7:1 | 1.2:1 | 1.4:1 | −0.9 | −1.1 | −1.1 | +26.5 | +22.7 | +30.3 |
| p23Δ5–45aa | 12:1 | 5.6:1 | 5:1 | +2.0 | +1.8 | +1.6 | +8.1 | +11.1 | +12.4 |
| p23Δ46–90aa | 1.5:1 | 1.1:1 | 1.1:1 | −0.8 | −1.0 | −1.2 | +27.2 | +25.8 | +33.7 |
| p23Δ91–180aa | 1.3:1 | 1.1:1 | 1.1:1 | −0.7 | −1.2 | −1.3 | +27.4 | +23.8 | +32.2 |
| p23Δ181–209aa | 35:1 | 16:1 | 28:1 | +2.0 | +2.0 | +1.3 | +3.1 | +3.8 | +2.8 |

While there were small effects on the accumulation of the positive-stranded sgRNA in these mutants, substantial increases in the accumulation of negative-stranded sgRNA were observed (Table 1). Deletion of amino acid codons 5 to 45 caused an increase in the accumulation of the positive-stranded sgRNA by ≈1- to 2-fold and negative-stranded sgRNA by ≈8 to 12-fold compared to CTV-p23 (Fig. 6B, compare a and c; Table 1). Deletion of amino acid codons 46 to 90 and 91 to 180 caused the greatest increase in the accumulation of negative-stranded sgRNA, approximately 24- to 34-fold, but the accumulation of the positive-stranded sgRNA was decreased by only 1- to 2-fold (Fig. 6B, compare d and e with a; Table 1). Mutant p23Δ180–209aa accumulated positive to negative strands at an approximately 16 to 35:1 ratio, similar to that of CTV-p23 (Fig. 6B, compare a and f; Table 1). The slight increase in the accumulation of negative-stranded sgRNA in p23Δ180–209aa can be attributed to an increase in the overall level of replication (Fig. 6B, f).

**Analysis of zinc finger domain in asymmetric accumulation of sgRNAs.** Deletion mutations in p23 suggested that amino acid residues 46 to 180 were critical for asymmetric accumulation of sgRNAs. The p23 protein was previously shown to contain an RNA-binding domain between amino acid residues 50 and 86, a region containing several basic amino acid residues and a putative zinc finger domain (15). The conserved cysteine and histidine amino acids are thought to be zinc-coordinating residues of a zinc finger domain. We examined the requirement for the zinc finger domain by replacing these cysteine and histidine residues with alanine. The two cysteine residues at positions 68 and 71 were replaced with alanines to obtain CTV-p23-$C^{68}A/C^{71}A$ (Fig. 7A). The histidine residue at position 75 and cysteine at position 85 were replaced with alanine residues to obtain CTV-p23-$H^{75}A$ and CTV-p23-$C^{85}A$, respectively (Fig. 7A). All of the mutants replicated efficiently in protoplasts. However, replacement of conserved cysteine residues with alanine resulted in a 12- to 15-fold increase in the accumulation of negative-stranded sgRNAs and a 1- to 2-fold decrease in positive-stranded sgRNAs (Fig. 7B, b and d). The replacement of the histidine residue with alanine had only a minor effect on asymmetry in sgRNA accumulation, accumulating plus- and minus-stranded sgRNAs similarly to the wild-type virus (Fig. 7B, c).

**p23 increases gene expression.** The above observations suggest that p23 regulates the accumulation of negative-stranded sgRNAs. It is possible that deletion of p23 results in an increase in double-stranded RNAs and a substantial decrease in

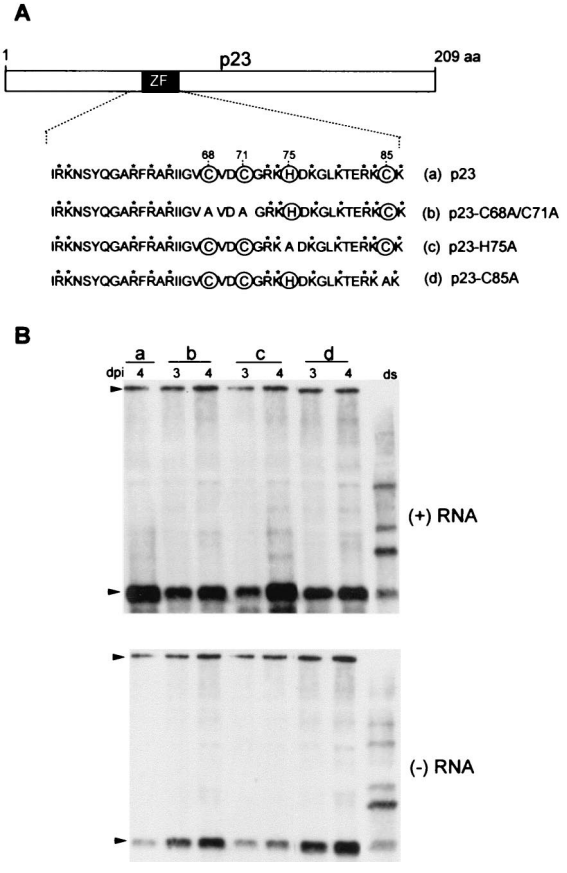


FIG. 7. Analysis of the zinc finger domain of p23 in asymmetric accumulation of sgRNAs. (A) Schematic diagram of p23 ORF with zinc finger domain (ZF). The amino acid sequences of the basic region and proposed zinc finger domain of p23 are shown. The conserved cysteine and histidine residues presumably bound to the zinc ions are circled, and basic amino acid residues are marked with asterisks. The positions of the conserved cysteine and histidine residues in the p23 protein are indicated. Point mutations were introduced to change C68 and C71 to alanine residues (p23-C68A/C71A), H75 to alanine (p23-H75A), and C85 to alanine (p23-C85A). (B) Northern blot analysis of accumulation of plus- and minus-stranded p23 sgRNAs from *N. benthamiana* protoplasts transfected with CTV-p23 (a) and mutants with alterations in the zinc finger domain (b to d) at 3 or 4 dpi. The blots were hybridized with 3′ positive- and negative-stranded RNA-specific riboprobes. Double-stranded RNA (ds) from CTV-infected plants was included in the Northern blot to equalize the strand-specific riboprobes. Genomic RNA and p23 sgRNA are indicated by arrowheads and arrows, respectively.

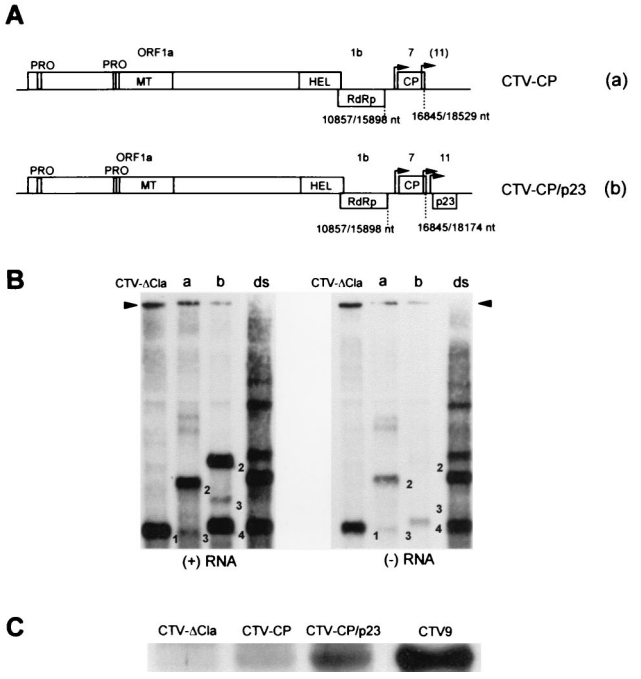


FIG. 8. Effect of p23 ORF on the expression of other genes. (A) Schematic diagrams of CTV-CP (a) and CTV-CP/p23 (b). Bent arrows represent the approximate positions of the 5′ termini of the sgRNAs driven by the controller element for the corresponding ORF. (B) Northern blot analysis of accumulation of positive- and negative-stranded RNAs from mesophyll protoplasts transfected with CTV-ΔCla, CTV-CP (a), and CTV-CP/p23 (b) at 4 dpi. The blots were hybridized with 3′ positive- and negative-stranded RNA-specific riboprobes, and double-stranded RNA (ds) was included in Northern blots to equalize the probes. 1, p33/p23 chimeric sgRNA produced under p33 controller element; 2, CP sgRNA; 3, p18 sgRNA produced from p18 sgRNA controller element present in the 3′ end of the CP ORF; 4, p23 sgRNA. (C) Western immunoblot analysis of CP from protoplasts transfected with CTV-ΔCla, CTV-CP, and CTV-CP/p23. Virions from wild-type CTV (CTV9) were used as a positive control.

single-stranded sgRNAs that could function as mRNAs. Therefore, we examined the effect of the p23 gene on the expression of the major coat protein (CP) gene in the presence and absence of p23 (CTV-CP/p23 and CTV-CP, respectively). The region between nt 15898 and 16845, comprising the intergenic region 5′ of the CP ORF that contained the sgRNA controller element (8) and the complete CP ORF, was inserted into CTV-ΔCla333 to obtain CTV-CP (Fig. 8A, a). CTV-CP contained the complete CP gene under its own promoter plus only the 3′ part of p23 ORF without its sgRNA controller element and was unable to express the p23 protein. CTV-CP/p23 contained complete CP and p23 genes (Fig. 8A, b).

Both CTV-CP and CTV-CP/p23 replicated efficiently and produced positive- and negative-stranded genomic and sgRNAs. CTV-CP produced the CP sgRNA and a truncated p18 sgRNA, whereas CTV-CP/p23 produced those plus the p23 sgRNA (Fig. 8B). The p18 sgRNA was produced because its controller element is located in the 3′ end of the CP ORF (8). The positive- and negative-stranded CP sgRNAs accumulated at ratios of 50:1 and 4.5:1 in the presence and absence of the p23 gene (CTV-CP/p23 and CTV-CP), respectively (Fig. 8B, compare a and b). The presence of the p23 ORF in CTV-CP/p23 resulted in a decrease in the accumulation of negative-stranded CP sgRNA of 11- to 17-fold and an increase in the accumulation of positive-stranded CP sgRNA of only 1- to 2-fold.

Total protein from CTV-CP- and CTV-CP/p23-inoculated protoplasts was analyzed by sodium dodecyl sulfate-polyacrylamide gel electrophoresis (SDS-PAGE), followed by a Western blot immunoassay using CP-specific polyclonal antibodies. The presence of the p23 ORF resulted in a substantial increase in the expression of CP by CTV-CP/p23, approximately 12- to 15-fold more than by CTV-CP (Fig. 8C).

## DISCUSSION

The positive- to negative-stranded RNA ratio of CTV RNAs, approximately 40 to 50:1, falls within the range of that of the genomic RNAs of most positive-stranded RNA viruses, particularly the more similar alphavirus supergroup and large complex viruses of the *Nidovirales*. However, we noticed that a CTV mutant with all of the 3′ genes deleted replicated efficiently but produced plus-to-minus strand ratios of genomic and sgRNA that were greatly altered, with almost as much negative-stranded RNAs as positive-stranded RNAs (22). By examining a series of mutants in this study, the cause of the altered ratio was mapped to the p23 gene. More precise mutations suggested that the p23 protein controlled the ratio of plus to minus strands of CTV. These data suggest that the p23 protein slightly increased the accumulation of plus strands but greatly decreased the accumulation of minus strands.

The loss of function due to a +1 frameshift after the fifth amino acid codon suggests that the p23 protein, not the RNA sequence, is responsible for the drastic upregulation of minus-stranded sgRNA accumulation. Examination of the sequences of p23 proteins from different strains of CTV showed remarkable conservation both of the basic region and of cysteine and histidine residues in a putative zinc finger domain, suggesting their functional importance (15). Zinc finger-containing proteins are ubiquitous proteins in eukaryotes that bind to nascent RNA, template DNA, or subunits of the transcriptional machinery (5). Our deletion analysis suggests that the N-terminal amino acids (5 to 45) and the C-terminal amino acids (181 to 209) were not absolutely required for the in vivo function of the p23 gene, whereas internal amino acids, including the zinc finger domain, were indispensable for asymmetric accumulation of plus- and minus-stranded sgRNAs.

The change of conserved Cys-68, Cys-71, and Cys-85 to Ala in p23 resulted in loss of asymmetric amplification, suggesting importance for the putative zinc finger domain in regulation of the ratio of positive- to negative-stranded RNAs. However, mutation of the His-75 to Ala had little effect. López et al. (15) demonstrated that the CTV p23 gene product binds RNA in vitro, with the RNA-binding domain mapping between amino acid residues 50 and 86, which include the putative zinc finger domain. However, mutation of the conserved cysteines and histidine in the putative zinc finger domain did not prevent RNA binding (15). These data suggest that the in vivo function of the p23 protein has greater requirements than RNA binding. Recently, Tijms et al. (33) reported that a zinc finger domain containing nsp1 of the nidovirus *Equine arteritis virus* is crucial for sgRNA synthesis. However, this protein is required

for sgRNA synthesis, whereas the CTV p23 protein appears only to reduce negative-strand accumulation.

The p21 gene product of *Beet yellows virus* (BYV), a related *Closterovirus*, is positionally analogous to the CTV p23 ORF and was reported to greatly affect replication of the viral RNAs (21). However, the BYV p21 gene and the CTV p23 gene appear to function very differently. Deletion of the p21 gene of BYV reduced RNA synthesis by ≈80%. In contrast, not only did deletion of the p23 gene of CTV have little effect on positive-stranded genomic RNA accumulation, as reported previously (22), it resulted in a net increase in total CTV viral RNA accumulation due to the increase in negative strands.

Because there is little information concerning mechanisms affecting positive-to-negative strand ratios of sgRNA, we can only compare CTV to mechanisms that control the ratio of positive to negative strands of genomic RNAs. The validity of this comparison is increased by the general similarity of the plus-to-minus ratios of CTV genomic and sgRNA for the different mutants (examine Fig. 1 to 8), even though we have difficulty quantifying the large genomic RNAs to calculate ratios.

Regulation of CTV genomic and sgRNA plus-to-minus ratios appears to differ considerably from those of the examined alpha-like viruses. In BMV, the change to asymmetrical replication due to the addition of RNA 3 to RNAs 1 and 2 results in a large amplification of genomic plus strands (16). A similar amplification of positive strands appeared to be induced by the AMV coat protein (34). A change in the replicase complex converts SIN replication from the symmetrical phase, which produces positive and negative strands of the genomic RNA in an approximately 1:1 ratio, to the asymmetrical phase, which produces exclusively positive strands (26, 27). A common feature of these systems is that mutation reduced the amount of positive strands produced with relatively little effect on production of negative strands. In contrast, in the absence of the p23 protein, CTV accumulated increased amounts of negative strands with little effect on positive strands.

It is not clear at this time why a virus would have a gene product to reduce negative-stranded RNA accumulation. It appears that the p23 protein serves as a switch to convert replication from symmetrical to asymmetrical production of positive- and negative-stranded RNAs. SIN does this by converting the replication complex from an unstable to a stable form (26). Perhaps the addition of the p23 protein to the CTV replication complex functions similarly, with the major difference being that the p23 protein did not appreciably amplify accumulation of the amount of positive strands. It is possible that the p23 protein, which has been shown to be an early protein (19), binds to the 3′ end of the positive-sense RNA to reduce the synthesis of negative strands.

A long-standing conundrum of virology has been the question of the in vivo relationship of complementary positive and negative strands of RNA: whether they exist in a double-stranded helix in the cell or only become double-stranded during extraction. The large amount of negative strands corresponding to the CTV RNAs revives the question of whether the positive-stranded sgRNAs are available as mRNAs in the presence of almost equal amounts of negative-stranded sgRNAs. We were able to examine this phenomenon by measuring protein synthesis in vivo from an mRNA with little cRNA compared to an mRNA with almost equal amounts of cRNA. The presence of the p23 gene resulted in an 11- to 17-fold decrease in the amount of minus strands of the CP sgRNA with only a ≈1- to 2-fold increase in positive strands, yet caused a 12- to 15-fold increase in the production of CP. The presence of complementary strands of the sgRNAs was associated with reduced translatability of those mRNAs, suggesting that they were made unavailable, perhaps as double-stranded RNAs. Thus, the p23 protein both reduces negative-stranded RNA accumulation and indirectly enhances gene expression.

## ACKNOWLEDGMENTS

We thank Cecile Robertson, Judy Harber, and John Cook for excellent technical assistance.

This research was supported in part by an endowment from the J. R. and Addie S. Graves family and grants from the Florida Citrus Production Research Advisory Council, the National Citrus Research Council, the U.S.-Israel BARD, USDA/ARS Cooperative Agreement, and the USDA/NRI. María A. Ayllón was supported by a postdoctoral fellowship from Ministerio de Educación y Ciencia (Spain).

## REFERENCES

1. **Adkins, S., S. S. Stawicki, G. Faurote, R. W. Siegel, and C. C. Kao.** 1998. Mechanistic analysis of RNA synthesis by RNA-dependent RNA polymerase from two promoters reveals similarities to DNA-dependent RNA polymerase. RNA **4:**455–470.
2. **Baric, R. S., and B. Yount.** 2000. Subgenomic negative-strand RNA function during mouse hepatitis virus infection. J. Virol. **74:**4039–4046.
3. **Buck, K. W.** 1996. Comparison of the replication of positive-stranded RNA viruses of plants and animals. Adv. Virus Res. **47:**159–251.
4. **Chambers, T. J., C. S. Hahn, R. Galler, and C. M. Rice.** 1990. Flavivirus genome organization, expression, and replication. Annu. Rev. Microbiol. **44:**649–688.
5. **Clarke, N. D., and J. M. Berg.** 1998. Zinc fingers in *Caenorhabditis elegans*: finding families and probing pathways. Science **282:**2018–2022.
6. **Dawson, W. O., and J. A. Dodds.** 1982. Characterization of sub-genomic double-stranded RNAs from virus-infected plants. Biochem. Biophys. Res. Commun. **107:**1230–1235.
7. **French, R., and P. Ahlquist.** 1987. Intercistronic as well as terminal sequences are required for efficient amplification of brome mosaic virus RNA3. J. Virol. **61:**1457–1465.
8. **Gowda, S., T. Satyanarayana, M. A. Ayllón, M. R. Albiach-Martí, M. Mawassi, S. Rabindran, S. M. Garnsey, and W. O. Dawson.** 2001. Characterization of the *cis*-acting elements controlling subgenomic mRNAs of citrus tristeza virus: production of positive- and negative-stranded 3′-terminal and positive-stranded 5′-terminal RNAs. Virology **286:**134–151.
9. **Hilf, M. E., A. V. Karasev, H. R. Pappu, D. J. Gumpf, C. L. Niblett, and S. M. Garnsey.** 1995. Characterization of citrus tristeza virus subgenomic RNAs in infected tissue. Virology **208:**576–582.
10. **Ho, S. N., H. D. Hunt, R. M. Horton, J. K. Pullen, and L. R. Pease.** 1989. Site-directed mutagenesis by overlap extension using polymerase chain reaction. Gene **77:**51–59.
11. **Karasev, A. V., V. P. Boyko, S. Gowda, O. V. Nikolaeva, M. E. Hilf, E. V. Koonin, C. L. Niblett, K. Cline, D. J. Gumpf, R. F. Lee, S. M. Garnsey, D. J. Lewandowski, and W. O. Dawson.** 1995. Complete sequence of the citrus tristeza virus RNA genome. Virology **208:**511–520.
12. **Karasev, A. V., M. E. Hilf, S. M. Garnsey, and W. O. Dawson.** 1997. Transcriptional strategy of closteroviruses: mapping the 5′ termini of the citrus tristeza virus subgenomic RNAs. J. Virol. **71:**6233–6236.
13. **Lai, M. M. C.** 1990. Coronavirus: organization, replication, and expression of genome. Annu. Rev. Microbiol. **44:**303–333.
14. **Lai, M. M. C., and D. Cavanagh.** 1997. The molecular biology of coronaviruses. Adv. Virus Res. **48:**1–100.
15. **López, C., J. Navas-Castillo, S. Gowda, P. Moreno, R. Flores.** 2000. The 23-kDa protein coded by the 3′-terminal gene of citrus tristeza virus is an RNA-binding protein. Virology **269:**462–470.
16. **Marsh, L. E., C. C. Huntley, G. P. Pogue, J. P. Connell, and T. C. Hall.** 1991. Regulation of (+):(-)-strand asymmetry in replication of brome mosaic virus RNA. Virology **182:**76–83.
17. **Miller, W. A., and G. Koev.** 2000. Synthesis of subgenomic RNAs by positive-strand RNA viruses. Virology **273:**1–8.
18. **Nassuth, A., and J. F. Bol.** 1983. Altered balance of the synthesis of plus- and minus-strand RNAs induced by RNAs 1 and 2 of alfalfa mosaic virus in the absence of RNA3. Virology **124:**75–85.

19. **Navas-Castillo, J., M. R. Albiach-Martí, S. Gowda, M. E. Hilf, S. M. Garnsey, and W. O. Dawson.** 1997. Kinetics of accumulation of citrus tristeza virus RNAs. Virology **228:**92–97.
20. **Pappu, H. R., A. V. Karasev, E. J. Anderson, S. S. Pappu, M. E. Hilf, V. J. Febres, R. M. G. Eckloff, M. McCaffery, V. P. Boyko, S. Gowda, V. V. Dolja, E. V. Koonin, D. J. Gumpf, K. C. Cline, S. M. Garnsey, W. O. Dawson, R. F. Lee, and C. L. Niblett.** 1994. Nucleotide sequence and organization of eight 3′ open reading frames of the citrus tristeza closterovirus genome. Virology **199:**35–46.
21. **Peremyslov, V. V., Y. Hagiwara, and V. V. Dolja.** 1998. Genes required for replication of the 15.5-kilobase RNA genome of a plant closterovirus. J. Virol. **72:**5870–5876.
22. **Satyanarayana, T., S. Gowda, V. P. Boyko, M. R. Albiach-Martí, M. Mawassi, J. Navas-Castillo, A. V. Karasev, V. Dolja, M. E. Hilf, D. J. Lewandowski, P. Moreno, M. Bar-Joseph, S. M. Garnsey, and W. O. Dawson.** 1999. An engineered closterovirus RNA replicon and analysis of heterologous terminal sequences for replication. Proc. Natl. Acad. Sci. USA **96:**7433–7438.
23. **Satyanarayana, T., S. Gowda, M. Mawassi, M. R. Albiach-Martí, M. A. Ayllón, C. Robertson, S. M. Garnsey, and W. O. Dawson.** 2000. Closterovirus encoded HSP70 homolog and p61 in addition to both coat proteins function in efficient virion assembly. Virology **278:**253–265.
24. **Satyanarayana, T., M. Bar-Joseph, M. Mawassi, M. R. Albiach-Martí, M. A. Ayllón, S. Gowda, M. E. Hilf, P. Moreno, S. M. Garnsey, and W. O. Dawson.** 2001. Amplification of citrus tristeza virus from a cDNA clone and infection of citrus trees. Virology **280:**87–96.
25. **Sawicki, S. G., and D. L. Sawicki.** 1990. Coronavirus transcription: Subgenomic mouse hepatitis virus replicative intermediates function in RNA synthesis. J. Virol. **64:**1050–1056.
26. **Sawicki, S. G., and D. L. Sawicki.** 1996. Sindbis virus RNA-negative mutants that fail to convert from minus-strand to plus-strand synthesis: role of the nsP2 protein. J. Virol. **70:**2706–2719.
27. **Sawicki, D. L., and S. G. Sawicki.** 1998. Role of the nonstructural polyproteins in alphavirus RNA synthesis. Adv. Exp. Med. Biol. **440:**187–198.
28. **Sawicki, D. L., and S. G. Sawicki.** 1998. A new model for coronavirus transcription. Adv. Exp. Med. Biol. **440:**215–219.
29. **Sawicki, D. L., T. Wang, and S. G. Sawicki.** 2001. The RNA structures engaged in replication and transcription of the A59 strain of mouse hepatitis virus. J. Gen. Virol. **82:**385–396.
30. **Sethna, P. B., S-L. Hung, and D. A. Brian.** 1989. Coronavirus subgenomic minus-strand RNAs and the potential for mRNA replicons. Proc. Natl. Acad. Sci. USA **86:**5626–5630.
31. **Siegel, R. W., L. Bellon, L. Beigelman, and C. C. Kao.** 1998. Moieties in an RNA promoter specifically recognized by a viral RNA-dependent RNA polymerase. Proc. Natl. Acad. Sci. USA **95:**11613–11618.
32. **Sit, T. L., A. A. Vaewhongs, and S. A. Lommel.** 1998. RNA mediated transactivation of transcription from a viral RNA. Science **281:**829–832.
33. **Tijms, M. A., L. C. van Dinten, A. E. Gorbalenya, and E. J. Snijder.** 2001. A zinc finger-containing papain-like protease couples subgenomic mRNA synthesis to genome translation in a positive-stranded RNA virus. Proc. Natl. Acad. Sci. USA **98:**1889–1894.
34. **van der Kuyl, A. C., L. Neeleman, and J. F. Bol.** 1991. Role of alfalfa mosaic virus coat protein in regulation of the balance between viral plus and minus strand RNA synthesis. Virology **185:**496–499.